

DEPTH DEPENDENCY OF STRESS PARAMETERS ON STRONG MOTION GENERATION AREAS FOR INLAND CRUSTAL EARTHQUAKES IN JAPAN

Ken Miyakoshi¹, Katsuhiko Kamae², and Kojiro Irikura³

¹Chief Researcher, Geo-Research Institute, Osaka, Japan

²Professor, Kyoto University Research Reactor Institute, Kumatori, Japan

³Professor, Aichi Institute of Technology, Toyota, Japan

Email: ken@geor.or.jp

ABSTRACT

The depth dependency of average static stress drop on asperities with large slip was presented by Asano and Iwata (2011). They used heterogeneous kinematic slip models estimated by waveform inversion analysis in the frequency range below 1Hz. We compiled the stress drops in SMGAs for nineteen recent crustal earthquakes (M_w 5.4-6.9) in Japan from 1995 to 2014, which are estimated by the empirical Green's function method in the frequency range 0.1-10Hz. The depth dependency of the stress drops in SMGAs is not clear due to their large variance. Next we compiled the acceleration source spectral-level ("acceleration level (A)") as stress parameter in SMGAs. The acceleration level (A) means the flat level of the acceleration source spectrum in Dan and Sato (1998), which is determined by stress drop and equivalent radius of SMGA. The acceleration level (A) in proportional to the one-third power of the seismic moment (Dan *et al.*, 2001) can be normalized by the one-third power of the seismic moment ("normalized A "). We examined the depth dependency of the normalized A . Referring to the regression line for the depth dependency of average static stress drop by Asano and Iwata (2011), we estimated the regression line of the normalized A in SMGAs. The regression line for the depth dependency of stress drop, which is converted from the regression line for the depth dependency of the normalized A , is a little higher than the empirical relationship of stress drop by Asano and Iwata (2011). Comparing observed seismograms with the simulated ones using forward simulation, we need to validate the depth dependency of stress drop and improve its accuracy for predicting high-accuracy strong ground motions for inland crustal earthquakes in Japan.

Keywords: stress drop, acceleration source spectrum, strong motion generation area (SMGA)

INTRODUCTION

Near-field ground motions are generally controlled by heterogeneities in the slip and stress drop distributions on the source fault. Consequently, it is important to characterize these heterogeneities of source models for the prediction of strong ground motion. After the 1995 Hyogo-ken Nanbu earthquake (M_w 6.9) in Japan, the dense strong ground motion networks (K-NET, KiK-net) were installed with about 20 km intervals by NIED (National Research Institute for Earth Science and Disaster Prevention). Using strong ground motions near the source region, high accuracy heterogeneous slip models are estimated by inversion analysis in the frequency range below 1Hz. Somerville *et al.* (1999) have proposed a quantitative criterion to extract the asperity area whose slip is 1.5 or more times larger than the average slip over the rupture area. They also proposed empirical scaling relationships based on waveform inversion results using strong motion data and teleseismic data of inland earthquakes occurring mostly in California, USA, but including a few in Japan. Based on broadband strong ground motion simulations using the empirical Green's function method (EGF method; Irikura, 1986) in the frequency range 0.1-10Hz, Miyake *et al.* (2003) found that the strong motion generation area (SMGA), which is defined as a high slip velocity or a high stress drop area on the rupture area, spatially coincides with the asperity area for inland crustal earthquakes.

Asano and Iwata (2011) pointed out the depth dependency of average static stress drop on asperities, and proposed the empirical relationship between the average static stress drop and its depth on

asperities. They used heterogeneous kinematic slip models estimated by waveform inversion analysis in the frequency range below 1Hz. The stress drops on the fault were estimated by spatiotemporal slip models obtained by the waveform inversion analysis. The average static stress drops on asperities are in the range 6-23 MPa.

On the other hand, the stress drops in SMGAs have been estimated by the EGF method in the frequency range 0.1-10Hz. We compiled the stress drops in SMGAs of nineteen recent crustal earthquakes (M_w 5.4-6.9) in Japan from 1995 to 2014. The depth dependency of the stress drops in SMGAs is not clear due to their large variance. Next we compiled the acceleration source spectral-level A (hereafter, "acceleration level (A)") as stress parameter in SMGAs. The acceleration level (A) means the flat level of the acceleration source spectrum in Dan and Sato (1998). The acceleration level (A) in proportional to the one-third power of the seismic moment (Dan *et al.*, 2001) can be normalized by the one-third power of the seismic moment (hereafter, "normalized A "). In this study, we examined the depth dependency of normalized A . As the results, we recognized the depth dependency of the normalized A in SMGAs as well as the average static stress drops on asperities (Asano and Iwata, 2011).

DEPTH DEPENDENCY OF THE STRESS DROPS IN SMAGS

SMGA models of nineteen crustal earthquakes (M_w 5.4-6.9) which occurred recently in Japan were compiled to examine the depth dependency of stress drops in SMGAs. Fig. 1 shows the epicenters of nineteen crustal earthquakes, with their focal mechanisms. These focal mechanisms are referred from the source mechanism information of F-net operated by NIED. Table 1 shows stress drop in SMGA and its centroid depth for the nineteen crustal earthquakes in this study. The centroid depths of SMGAs are in the range 3-15 km and stress drops in the range 1-47 MPa. Fig.2 shows an example for the SMGA model of the 2013 Tochigi hokubu earthquake (EQ.16) referred to by Somei *et al.* (2014). Red and black solid rectangles show SMGA and asperity area respectively. Asperity area with large slip is also identified by the criterion of Somerville *et al.* (1999). It is recognized that asperity area and SMGA occupy almost the same regions in Fig.2. Fig.3 shows the relationship between area of SMGA and seismic moment (M_o). The empirical relationship between the combined area of asperities and seismic moment ($Sa-M_o$; Somerville *et al.*, 1999) is also plotted in this figure. We recognized that areas of SMGAs are consistent with the empirical scaling relationship ($Sa-M_o$) by Somerville *et al.* (1999).

Table 1. Source parameters in SMGAs and centroid depths of inland crustal earthquakes examined in this study.

No.	EQ. NAME	Mo(F-net) (Nm)	Mech. ²⁾	Surface ³⁾ or Buried	Reference	Total SMGA km ²	Num. of SMGA	SMGA (km ²)			Centroid Depth (km)			Stress drop (MPa)			
								SMGA1	SMGA2	SMGA3	SMGA1	SMGA2	SMGA3	SMGA1	SMGA2	SMGA3	
EQ.1	1995 Hyogo nanbu	3.30E+19 ¹⁾	SS	Buried	[11] Kamae & Irikura (1998)	304.0	3	176.0	64.0	64.0	7.9	12.0	9.0	8.6	16.3	8.6	
EQ.2	2008 Iwate-Miyagi nairiku	2.72E+19	RV	Surface	[12] Kamae (2008)	102.2	2	92.5	46.2	46.2	5.7	12.3		13.8	13.8		
					[13] Kurahashi <i>et al.</i> (2014)			113.0	91.1	21.9	3.1	6.6		12.8	16.7		
EQ.3	2007 Noto hanto	1.36E+19	RV	Buried	[14] Kurahashi <i>et al.</i> (2008a)	85.0	3	52.7	39.7	13.0	8.7	4.3		25.8	10.3		
					[15] Maeda <i>et al.</i> (2008)			69.2	27.0	27.0	15.2	9.8	13.3	12.4	46.9	37.5	46.9
					[16] Yoshimi & Yoshida (2008)			146.0	98.0	48.0	8.7	12.7		9.4	15.6		
					[17] Ikeda <i>et al.</i> (2011)			97.9	51.8	23.0	23.0	7.67	4.39	5.48	20.0	20.0	10.0
EQ.4	2011 Fukushima hamadori	9.58E+18	NM	Surface	[18] Somei <i>et al.</i> (2011)	86.0	2	79.0	39.5	39.5	6.0	5.7		14.6	14.6		
					[19] Somei <i>et al.</i> (2015a)			93.6	54.7	38.9	4.9	10.9		10.0	15.8		
EQ.5	2007 Niigata chuetsu-oki	9.30E+18	RV	Buried	[10] Kurahashi <i>et al.</i> (2008b)	89.0	3	85.9	30.3	30.3	25.4	10.0	8.9	11.3	23.7	23.7	19.8
					[11] Yamamoto & Takenaka (2009)			92.3	36.0	36.0	20.3	6.3	5.4	6.9	19.5	14.8	19.5
EQ.6	2000 Tottori seiho	8.62E+18	SS	Buried	[12] Ikeda <i>et al.</i> (2002)	57.6	2	28.8	28.8		8.6	3.2		28.0	14.0		
EQ.7	2005 Fukuoka seiho-oki	7.80E+18	SS	Buried	[13] Suzuki & Iwata (2006)	41.8	1	41.8			6.8			10.7			
EQ.8	2004 Niigata chuetsu	7.53E+18	RV	Buried	[14] Kamae <i>et al.</i> (2005)	91.0	2	75.0	16.0		9.2	10.7		7.0	20.0		
EQ.9	2014 Niigata hokubu	2.76E+18	RV	Surface	[15] NRA report (2015)	59.9	1	59.9			4.5			9.4			
EQ.10	2011 Niigata-Niigata	2.13E+18	RV	Buried	[16] Somei <i>et al.</i> (2015a)	38.0	2	20.0	18.0		7.5	7.2		12.6	18.2		
EQ.11	March 1997 Kagoshima hokuseibu	1.40E+18	SS	Buried	[17] Miyake <i>et al.</i> (2003)	42.0	1	42.0			5.8			17.0			
EQ.12	May 1997 Kagoshima hokuseibu	1.22E+18	SS	Buried	[18] Miyake <i>et al.</i> (2003)	34.0	2	12.0	12.0		6.2	6.2		23.9	23.9		
EQ.13	2011 Shizuoka tobu	8.38E+17	SS	Buried	[19] Somei <i>et al.</i> (2012)	26.6	1	26.6			12.5			16.9			
EQ.14	1998 Iwate nairiku hokubu	7.53E+17	RV	Buried	[20] Miyake <i>et al.</i> (2003)	16.0	1	16.0			8.6			20.3			
EQ.15	1997 Yamaguchi hokubu	5.66E+17	SS	Buried	[21] Miyake <i>et al.</i> (2003)	14.4	1	14.4			6.8			20.5			
EQ.16	2013 Tochigi hokubu	5.54E+17	SS	Buried	[22] Somei <i>et al.</i> (2014)	17.6	1	17.6			3.1			16.4			
					[23] Kurahashi (2014)			8.1	8.1		14.8		9.0				
EQ.17	2013 Awaji island (Hyogo)	5.47E+17	RV	Buried	[24] Somei <i>et al.</i> (2015b)	10.0	1	12.3			12.1			11.2			
EQ.18	2004 Rumei (Hokkaido)	4.44E+17	RV	Buried	[25] Maeda & Sasatani(2009)	9.8	2	7.8	2.0		4.20	5.30		12.9	27.9		
EQ.19	2005 Fukuoka seiho-oki (Max. aftershock)	1.31E+17	SS	Buried	[26] Suzuki & Iwata (2006)	15.8	1	15.8			12.0			1.4			

1) Seismic moment is from Sekiguchi *et al.* (2002) 2) SS: Strike slip, RV: Reverse slip, NM: Normal slip

3) Information is from Yoshida *et al.* (2016)

* Information is from personal communication.

Centroid depth in italic is estimated from a figure of SMGA model in papers.

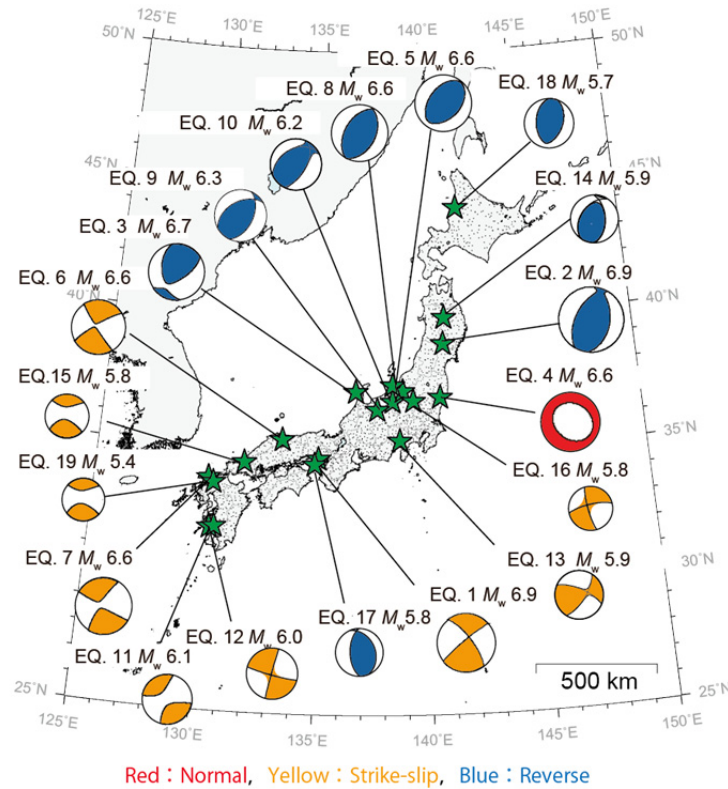


Figure 1. Distribution of 19 crustal events in Japan examined in this study and their focal mechanisms (F-net).

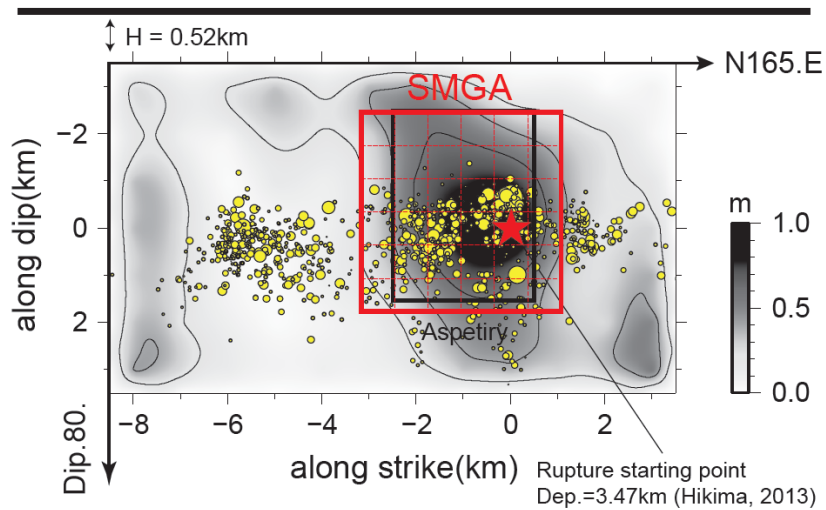


Figure 2. Example for the SMGA model for the 2013 Tohoku earthquake (EQ.16) referred to by Somei *et al.* (2014). SMGA with large slip velocity and asperity area with large slip are indicated by red and black solid rectangles, respectively.

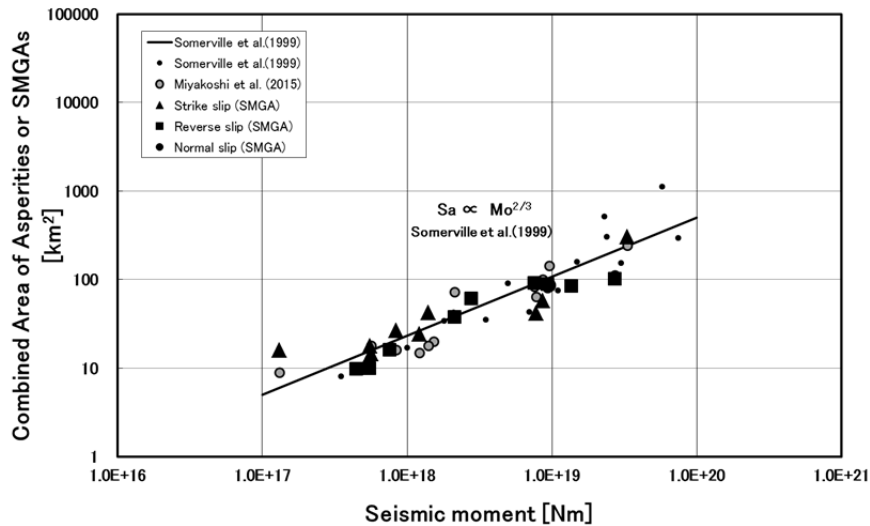


Figure 3. Relationship between area of SMGAs and seismic moment. Combined areas of asperities (Somerville *et al*, 1999; Miyakoshi *et al*, 2015) are also plotted. Solid line shows the empirical scaling relationship between the combined areas of asperities and seismic moment by Somerville *et al.* (1999).

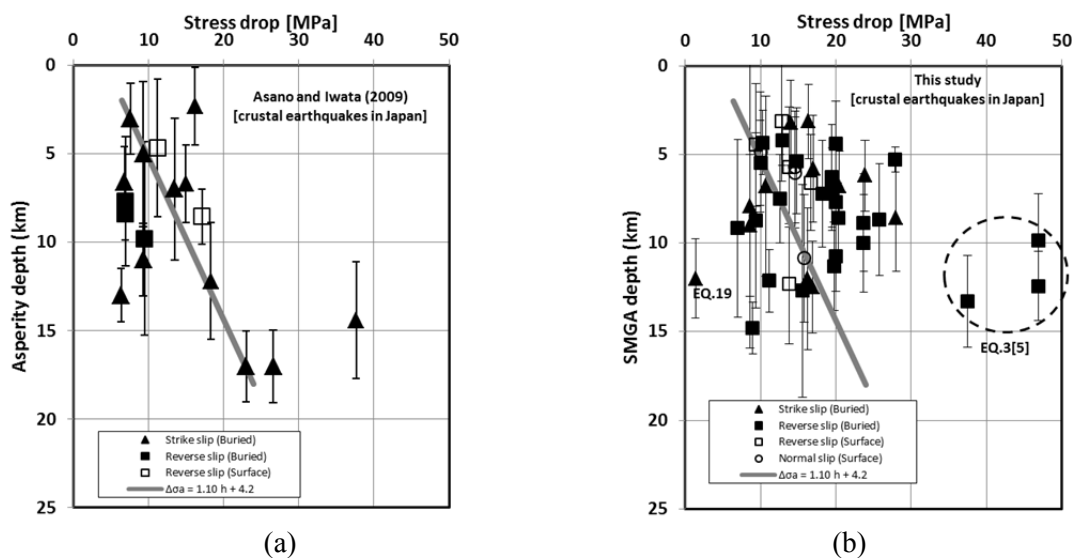


Figure 4(a). Relationship between the average static stress drop on asperities and its depth for inland crustal earthquakes in Japan (Asano and Iwata, 2011). (b) Relationship between stress drop in SMGAs and its depth for nineteen earthquakes examined in this study. Solid gray line shows the regression line for the depth dependency of average static stress drop (Eq.6; Asano and Iwata, 2011). Vertical bar shows the width of asperity area or SMGA. An open symbol indicates the surface breaking fault type, and a solid one indicates the buried fault type referred to by Yoshida *et al.* (2016).

Fig.4 (a) shows the depth dependency of average static stress drops on asperities (Asano and Iwata, 2011). Fig.4 (b) shows the depth dependencies of the stress drops in SMGAs for nineteen crustal earthquakes examined in Japan. It is clear that the variances of stress drops in SMGAs are larger than those on asperities. There is particularly large divergence for the stress drops of the 2007 Noto earthquake (EQ.3 [5] in Table 1) and the maximum aftershock for the 2005 Fukuoka seiho-oki (EQ.19 in Table 1) as shown in Fig.4 (b). The depth dependencies of the stress drops in SMGAs were not obvious due to their large variances.

ACCELERATION SOURCE SPECTRAL-LEVEL FROM SMGAS

Acceleration level (A) is represented theoretically by Madariaga (1979) as:

$$A_M = 4\pi\beta v_R \left\{ \sum_{i=1}^N (\Delta\sigma_i r_i)^2 \right\}^{\frac{1}{2}} \quad (1)$$

where β [m/s] is the S-wave velocity of the medium in the source region. v_R [m/s] is the rupture velocity in fault. $\Delta\sigma_i$ [MPa] is the stress drop in each SMGA. r_i [m] is equivalent radius for the each area of SMGA. i means i -th SMGA. The acceleration level (A [Nm/s²]) is determined by stress drop ($\Delta\sigma$) and equivalent radius (r) for SMGA. This means the area of SMGA and its stress drop may be in a relationship of trade-off. So it is expected that the acceleration level (A) as stress parameter is a more robust parameter than stress drop in SMGA. Next we examined the depth dependency of the acceleration level (A) in SMGA. Table 2 shows the acceleration level (A) and seismic moment for the nineteen crustal earthquakes in Japan. The S-wave velocity (β) and the rupture velocity (v_R) is also shown in this table. Geller (1976) showed the empirical relationship between the S-wave velocity (β) and the rupture velocity (v_R) as $v_R = 0.72 \beta$. Miyakoshi and Petukhin (2005) also showed the same empirical relationship as $v_R = 0.73 \beta$. Their results are compiled by waveform inversion analysis. However, the average ratio of the rupture velocity to the S-wave velocity (v_R/β) in the EGF method is 0.79 (sd. = 0.08) as shown in Table 2. This ratio (0.79) is larger than previous inversion results (0.72 or 0.73) by Geller (1976) or Miyakoshi and Petukhin (2005). The validation of this ratio should be investigated carefully as well as minutely based on each result in the EGF method.

Table 2. Acceleration level (A_D) and normalized A_M .

No.	EQ. NAME	Mo (F-net) (Nm)	Reference	β (km/s)	v_R (km/s)	v_R/β	A_0 (Nm/s ²) Dan et al.(2001)	A_N (Normalized A_M) at each SMGA [(Nm/s ²) ^{3/5}]		
								SMGA1	SMGA2	SMGA3
EQ.1	1995 Hyogo nanbu	3.30E+19 ¹⁾	[1]	3.50	2.80	0.80	1.62E+19	2.79E+12	5.29E+12	2.79E+12
EQ.2	2008 Iwate-Miyagi nairiku	2.72E+19	[2]	3.50	2.70	0.77	1.15E+19	2.63E+12	2.63E+12	
			[3]	3.40	2.80	0.82	1.19E+19	2.85E+12	3.71E+12	
EQ.3	2007 Noto hanto	1.36E+19	[4]	3.40 ²⁾	3.10	0.91	1.37E+19	5.39E+12	2.15E+12	
			[5]	3.50	2.80	0.80	3.14E+19	9.53E+12	7.62E+12	9.53E+12
			[6]	3.50	2.80	0.80	1.24E+19	3.00E+12	4.96E+12	
			[7]	3.50	2.50	0.71	1.56E+19	4.37E+12	4.37E+12	2.19E+12
EQ.4	2011 Fukushima hamadori	9.58E+18	[8]	3.40	2.90	0.85	1.06E+19	3.81E+12	3.81E+12	
			[9]	3.30	2.80	0.85	9.51E+18	2.67E+12	4.21E+12	
EQ.5	2007 Niigata chuetsu-oki	9.30E+18	[10]	3.40	2.70	0.79	1.72E+19	5.67E+12	5.67E+12	4.73E+12
			[11]	3.40	2.80 ³⁾	0.82	1.40E+19	5.04E+12	3.83E+12	5.04E+12
EQ.6	2000 Tottori seibu	8.62E+18	[12]	3.50	2.80 ³⁾	0.80	1.46E+19	6.42E+12	3.21E+12	
EQ.7	2005 Fukuoka seho-oki	7.80E+18	[13]	3.50	3.15	0.90	6.01E+18	2.73E+12		
EQ.8	2004 Niigata chuetsu	7.53E+18	[14]	3.50	2.00	0.57	8.72E+18	1.58E+12	4.53E+12	
EQ.9	2014 Nagano hokubu	2.76E+18	[15]	3.30	2.30	0.70	5.62E+18	2.79E+12		
EQ.10	2011Nagano-Niigata	2.13E+18	[16]	3.50	2.50	0.71	8.30E+18	3.34E+12	4.82E+12	
EQ.11	March 1997 Kagoshima hokuseibu	1.40E+18	[17]	3.10	2.50	0.81	7.51E+18	5.41E+12		
EQ.12	May 1997 Kagoshima hokuseibu	1.22E+18	[18]	3.10	2.30	0.74	7.98E+18	4.93E+12	4.93E+12	
EQ.13	2011Shizuoka tobu	8.38E+17	[19]	3.44	2.80	0.81	7.32E+18	6.32E+12		
EQ.14	1998 Iwate nairiku hokubu	7.53E+17	[20]	3.50	3.15	0.90	7.05E+18	6.98E+12		
EQ.15	1997 Yamaguchi hokubu	5.66E+17	[21]	3.10	2.79	0.90	5.30E+18	5.77E+12		
EQ.16	2013 Tochigi hokubu	5.54E+17	[22]	3.44	2.40	0.70	5.77E+18	4.90E+12		
EQ.17	2013 Awaji island (Hyogo)	5.47E+17	[23]	3.40	2.64	0.78	2.10E+18	2.00E+12		
			[24]	3.40	2.40	0.71	3.21E+18	2.77E+12		
EQ.18	2004 Rumbi (Hokkaido)	4.44E+17	[25]	3.00	2.70	0.90	3.39E+18	2.83E+12	6.12E+12	
EQ.19	2005 Fukuoka seho-oki (Max. aftershock)	1.31E+17	[26]	3.50	2.45	0.70	4.83E+17	6.65E+11		

- 1) Seismic moment is from Sekiguchi *et al.* (2002).
2) Rupture velocity in Asperity 2 and Asperity 3.
3) Rupture velocity in Asperity 1.
* Information is from personal communication.

Dan *et al.* (2001) proposed the empirical relationship between seismic moment and the acceleration level (Eq.2).

$$A_D \text{ [Nm/s]} = 2.46 \times 10^{10} \times (\text{Mo [Nm]} \times 10^7)^{1/3} \quad (2)$$

For the first step, we compared the acceleration level (A_D) of SMGAs of nineteen crustal earthquakes with the empirical relationship (Eq.2) by Dan *et al.* (2001).

$$A_D = 4\pi\beta^2 \left\{ \sum_{i=1}^N (\Delta\sigma_i r_i)^2 \right\}^{\frac{1}{2}} \quad (3)$$

They assumed an empirical equation proposed by Brune (1970) to evaluate the acceleration level (A_D , as shown in Eq.3), so the acceleration level (A_M , as shown in Eq.1) of Madariaga (1979) in this study

is around 0.79 times (due to $v_R = 0.79 \beta$), smaller than that of Dan *et al.* (2001). To compare the acceleration level (A_D) of SMGAs in this study and the empirical relationship (Eq.2) of Dan *et al.* (2001), we re-calculate the acceleration level (A_D) according to Eq.3. The re-calculated acceleration level (A_D) is also shown in Table 2. Fig.5 shows the relationship between the acceleration level (A_D) and seismic moment (Mo). The acceleration levels (A_D) of eighteen crustal earthquakes, excepting EQ.19, have good agreement with the empirical relationship by Dan *et al.* (2001). EQ.19 is the maximum aftershock of the 2005 Fukuoka seiho-oki earthquake, and its stress drop (1.4MPa) is considerably smaller than those of other earthquakes (see Table 1 or Fig.4 (b)). It is suggested that the breakage of source scaling could be caused by the difference in source characteristics between the aftershock and mainshocks. So we exclude EQ.19 for subsequent discussion.

For the second step, we calculated the acceleration level (A_{Mi}) of eighteen crustal earthquakes according to Eq.1 in each SMGA. Then the acceleration level (A_{Mi}) was normalized by the one-third power of weighted seismic moment (Mo_i) with reference to Eq. 5.

$$A_{Ni} = A_{Mi} / Mo_i^{1/3} \quad (4)$$

$$Mo_i = Mo \cdot S_{ai}^{3/2} / \sum_{i=1}^N S_{ai}^{3/2} \quad (5)$$

where Mo_i [Nm]: weighted seismic moment of i -th SMGA, S_{ai} [m²]: area of i -th SMGA, and A_N [(Nm)^{2/3}/s²]: normalized A_M .

Here, we used the conventional Eq.5 that is obtained by assuming the same stress drop in each SMGA, although Table 1 shows a little different stress drop in each SMGA. A list of normalized A_M for each SMGA in this study is shown in Table 2. Fig.6 shows the normalized A_M of eighteen crustal earthquakes. There is not a large divergence of the normalized A_M for the 2007 Noto earthquake (EQ.3 [5]) from other earthquakes.

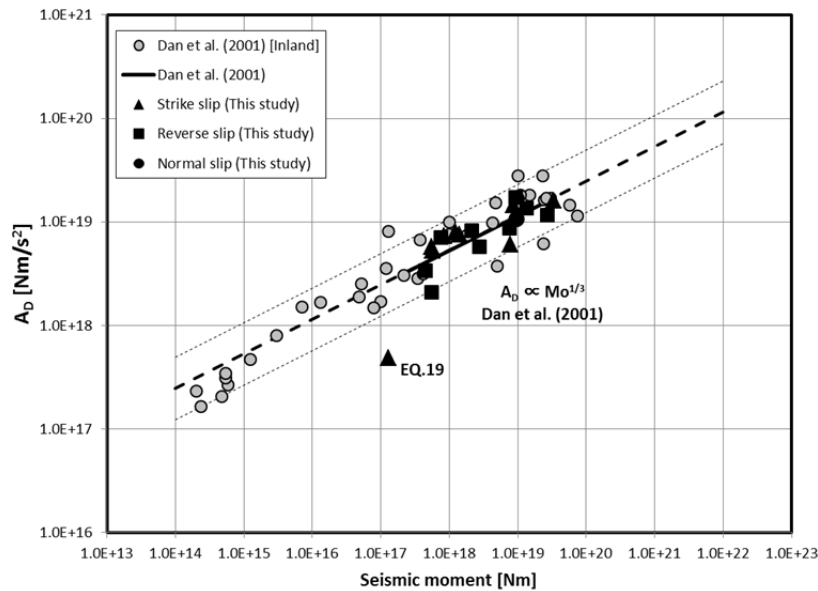


Figure 5. Relationship between the acceleration level (A_D) and seismic moment (Mo) for nineteen crustal earthquakes in Japan. Solid line and broken line show the empirical relationship between A_D and Mo by Dan *et al.* (2001). Gray solid circles denote the acceleration levels (A_D) by Dan *et al.* (2001), excepting subduction-zone earthquakes.

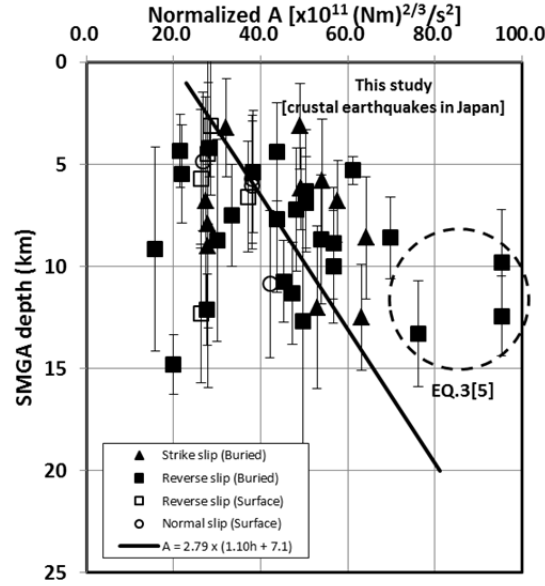


Figure 6. Relationship between A_N and its depth in SMGA for eighteen crustal earthquakes examined in this study. Vertical bar shows the width of SMGA for each event. Solid line shows the estimated regression line for the depth dependency of A_N in SMGA (Eq.10).

For the third step, we estimated the regression line for the depth dependency of the normalized A_M in SMGA. Here, we used the slope (1.1MPa/km) of the regression line for the depth dependency of average static stress drop on asperities (Eq.6; Asano and Iwata, 2011).

$$\Delta\sigma_a = 1.10 \times h + 4.2 \quad (\text{Japanese crustal earthquakes, Asano and Iwata, 2011}) \quad (6)$$

where $\Delta\sigma_a$ [MPa]: average static stress drop on asperity, h [km]: center depth of asperity.

In order to estimate the equivalent radius (r) for the area of asperity (see Eq.1), we used the next two assumptions:

$$S = 2.23 \times 10^{-15} \times (Mo \times 10^7)^{2/3} \quad (\text{Somerville } et al., 1999) \quad (7)$$

where S [km²]: rupture area, Mo [Nm]: seismic moment, and

$$S_a / S = 0.16 \quad (\text{Miyakoshi } et al., 2015) \quad (8)$$

where S_a [km²]: combined area of asperities, S [km²]: rupture area.

Eq.7 is the empirical scaling relationship for the 1st.-stage between the rupture area and the seismic moment by Somerville *et al.* (1999) and convenient for the seismic moment range lower than 7.5×10^{18} [Nm] ($M_w < 6.5$) (Irikura and Miyake, 2001). We used this scaling relationship, although the range of seismic moment for earthquakes used in this study is from 1.3×10^{17} to 3.3×10^{19} [Nm] (M_w 5.4-6.9). Eq.8 is obtained by the waveform inversion results of crustal earthquakes in Japan by Miyakoshi *et al.* (2015). We calculated the equivalent radius (r) for the area of asperity using Eqs. 7 and 8. We obtained the regression line (Eq.9) for the depth dependency of the normalized A_M on asperities using Eqs. 1 and 6 with assumption $\beta = 3.5$ km/s and $v_R = 0.79\beta$.

$$A_N = 2.79 \times (1.10 \times h + 4.2) \times 10^{11} \quad (9)$$

where A_N [(Nm)^{2/3}/s²]: normalized A_M , h [km]: centroid depth of asperity.

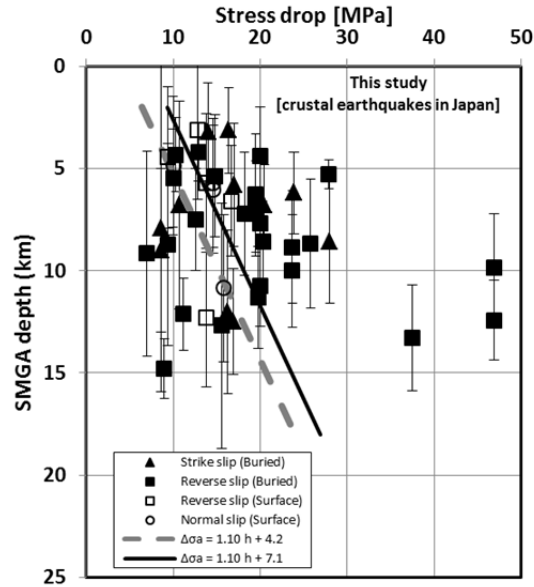


Figure 7. Relationship between stress drop and its depth in SMGA for eighteen crustal earthquakes examined in this study. Solid line shows the converted regression line for the depth dependency of stress drop (Eq.11). Gray broken line shows the regression line for the depth dependency of average static stress drop (Eq.6; Asano and Iwata, 2011).

Finally we estimated the regression line for the depth dependency of A_N in SMGA. Depth dependency of A_N was conveniently modeled as $A_N = 2.79 \times (1.10 \times h + b) \times 10^{11}$ with reference to Eq.9. After all, we obtained 7.1 as b for the regression line for the depth dependency of A_N in SMGA by the least squares method.

$$A_N = 2.79 \times (1.10 \times h + 7.1) \times 10^{11} \quad (10)$$

Solid line in Fig.6 shows the estimated regression line for the depth dependency of A_N in SMGA (Eq.10). The estimated regression line coincided with the relationship between A_N and its depth in SMGA for eighteen crustal earthquakes in Japan. Therefore, we converted the regression line for the depth dependency of A_N to stress drop as:

$$\Delta\sigma_{SMGA} = 1.10 \times h + 7.1 \quad (11)$$

where $\Delta\sigma_{SMGA}$ [MPa]: stress drop in SMGA, h [km]: centroid depth of SMGA.

Fig.7 shows the converted regression line for the depth dependency stress drop in SMGA (Eq.11) with comparison of another one (Eq.6; Asano and Iwata, 2011). The converted regression line for the stress drop in this study is a little higher than that by Asano and Iwata (2011).

CONCLUSIONS

We compiled SMGA models of nineteen crustal earthquakes (M_w 5.4-6.9) which occurred recently in Japan to examine the depth dependency of stress drops on SMGAs. However, we could not clearly recognize the depth dependency of the stress drops in SMGAs due to their large variances. So we compiled the acceleration source spectral-level A ("acceleration level (A)") as stress parameter, and examined the depth dependency of the acceleration level (A). Because the acceleration level (A) is proportional to the one-third power of the seismic moment (Dan *et al.*, 2001), the acceleration level (A) is normalized by the one-third power of the seismic moment ("normalized A "). We recognized the depth dependency of the normalized A for the inland crustal earthquakes in this study. Referring to the regression line for the depth dependency of average static stress drop on asperity by Asano and Iwata

(2011), we estimated the regression line for the depth dependency of the normalized A (A_N) in SMGA using the least squares method. The estimated regression line coincides with the relationship between the normalized A (A_N) and its depth in SMGA for inland crustal earthquakes examined in this study. The regression line for the depth dependency of stress drop, which is converted from the regression line for the depth dependency of the normalized A (A_N), is a little higher than that by Asano and Iwata (2011). Comparing observed seismograms with the simulated ones using forward simulation, we need to validate the depth dependency of stress drop and improve its accuracy for predicting high-accuracy strong ground motions for inland crustal earthquakes in Japan.

ACKNOWLEDGMENTS

We used the hypocentral information catalog of JMA (Japan Meteorological Agency), and the source information by F-net provided by NIED (National Research Institute for Earth Science and Disaster Prevention). We would like to thank Dr. Asano (DPRI) and Prof. Iwata (DPRI) for provision of the data set of the depth dependence of average stress drop on asperities. Dr. Kurahashi (AIT), Prof. Ikeda (NUT), and Dr. Maeda (NIED) for provision of the EGF modeling. Dr. Dan (ORI) provided the dataset of the acceleration source levels. This study was based on the 2015 research project "Improvement for uncertainty of strong ground motion prediction" by the Nuclear Regulation Authority (NRA), Japan.

REFERENCES

- Asano, K. and T. Iwata (2011). "Characterization of Stress Drops on Asperities estimated from the Heterogeneous Kinematic Slip Model for Strong Motion Prediction for Inland Crustal Earthquakes in Japan," *Pure and Applied Geophys.*, **168**, 105-116.
- Brune, J. N. (1970). "Tectonic Stress and the Spectra of Seismic Shear Waves from Earthquakes," *Journal of Geophysical Research*, **75**, 4997-5009.
- Dan, K. and T. Sato (1998). "Strong-Motion Prediction by Semi-Empirical Method based on Variable-Slip Rupture Model of Earthquake Fault," *J. Struct. Constr. Eng.*, AIJ, **509**, 49-60 (in Japanese).
- Dan, K., M. Watanabe, T. Sato and T. Ishii (2001). "Short-Period Source Spectra inferred from Variable-Slip Rupture Models and Modeling of Earthquake Faults for Strong Motion Prediction by Semi-Empirical Method," *J. Struct. Constr. Eng.*, AIJ, **545**, 51-62 (in Japanese).
- Geller, R. J. (1976). "Scaling Relations for Earthquake Source Parameters and Magnitude," *Bull. Seism. Soc. Am.*, **66**, 1501-1523.
- Ikeda, T., K. Kamae, S. Miwa and K. Irikura (2002). "Source Characterization and Strong Ground Motion Simulation of the 2000 Tottori-ken Seibu Earthquake using the Empirical Green's Function Method," *J. Struct. Constr. Eng.*, AIJ, **561**, 37-45 (in Japanese).
- Ikeda, T., K. Kamae and S. Miwa (2011). "Source modeling using the empirical Green's function method and strong ground motion estimation considering nonlinear site effect: An application to the 2005 West off Fukuoka prefecture earthquake and the 2007 Noto Hanto earthquake," *J. Struct. Constr. Eng.*, AIJ, **665**, 1253-1261 (in Japanese).
- Irikura, K. (1986). "Prediction of Strong Acceleration Motion using Empirical Green's Function," *7th Jpn. Earthq. Eng. Symp.*, 151-156.
- Kamae, K. and K. Irikura (1998). "Source Model of the 1995 Hyogo-ken Nanbu Earthquake and Simulation of Near-Source Ground Motion," *Bull. Seism. Soc. Am.*, **88**, 400-412.
- Kamae, K., T. Ikeda and S. Miwa (2005). "Source Model composed of Asperities for the 2004 Mid Niigata Prefecture, Japan, Earthquake ($M_{JMA}=6.8$) by the Forward Modeling using the Empirical Green's Function Method," *Earth Planets Space*, **57**, 533-538.
- Kamae, K. (2008). "Source Model of the 2008 Iwate-Miyagi Nairiku Earthquake (M_J 7.2) for Estimating Broad-Band Strong Ground Motion," (in Japanese). http://www.rrl.kyoto-u.ac.jp/jishin/iwate_miyagi_1.html
- Kurahashi, S., K. Masaki and K. Irikura (2008a). "Source Model of the 2007 Noto-Hanto Earthquake (M_W 6.7) for Estimating Broad-Band Strong Ground Motion," *Earth Planets Space*, **60**, 89-94.

- Kurahashi, S. K. Masaki, K. Miyakoshi and K. Irikura (2008b). "Source Model of the 2007 Niigata-ken Chuetsu-oki Earthquake using Empirical Green's Function (SE-Dip Model)," Japan Geoscience Union, S146-P017.
- Kurahashi, S., K. Irikura, K. Yoshida and K. Miyakoshi (2014). "Slip Velocity Time Function for Predicting Broadband Strong-Ground Motions from Inland Crustal Earthquakes," Seismological Society of Japan, S15-P20 (in Japanese).
- Kurahashi, S. (2014). "Source Model of the 2013 Awaji Island Earthquake (M_j 6.3) by using the Empirical Green's Function Method," personal com.
- Madariaga, R. (1979). "On the Relation between Seismic Moment and Stress Drop in the Presence of Stress and Strength Heterogeneity," *Journal of Geophysical Research*, **85**, 2243-2250.
- Maeda, T., M. Ichiyana, H. Takahashi, R. Honda, T. Yamaguchi, M. Kasahara and T. Sasatani (2008). "Source Parameters of the 2007 Noto Hanto Earthquake Sequence derived from Strong Motion Records at Temporary and Permanent Stations," *Earth Planets Space*, **60**, 1011-1016.
- Maeda, T. and T. Sasatani (2009). Strong Motions from an M_j 6.1 Inland Crustal Earthquake in Hokkaido, Japan: the 2004 Rumoi Earthquake," *Earth Planets Space*, **61**, 689-701.
- Miyake, H., T. Iwata and K. Irikura (2003). "Source Characterization for Broadband Ground-Motion Simulation: Kinematic Heterogeneous Source Model and Strong Motion Generation Area," *Bull. Seism. Soc. Am.*, **93**, 2531-2545.
- Miyakoshi, K. and A. Petukhin (2005). "Delineation of Rupture Velocity of Heterogeneous Source Model extracted from Source Inversion Results of Inland Earthquakes," Japan Geoscience Union, S046-P002 (in Japanese).
- Miyakoshi, K., K. Kamae and K. Irikura (2015). "Re-Examination of Scaling Relationships of Source Parameters of the Inland Earthquakes in Japan based on the Waveform Inversion of Strong Motion Data," *Journal of Japan Association for Earthquake Engineering*, **15**, 141-156 (in Japanese).
- NRA report (2015). "Source Model of the 2014 Nagano Hokubu Earthquake (M_j 6.7) by using the Empirical Green's Function Method," the 2015 research project "Improvement for uncertainty of strong ground motion prediction" by the Nuclear Regulation Authority (NRA).
- Sekiguchi, H., K. Irikura and T. Iwata (2002). "Source Inversion for Estimating the Continuous Slip Distribution on a Fault-introduction of Green's Functions Convolved with a Correction Function to Give Moving Dislocation Effects in Subfaults," *Geophys. J. Int.*, **150**, 377-391.
- Somei, K., M. Miyakoshi and K. Irikura (2011). "Estimation of Source Model and Strong Motion Simulation for the 2011 East Fukushima Prefecture Earthquake using the Empirical Green's Function Method," Seismological Society of Japan, P2-29 (in Japanese).
- Somei, K., K. Miyakoshi and K. Kamae (2012). "Source Model of the 2011 East Shizuoka Prefecture, Japan, Earthquake by using the Empirical Green's Function Method," Japan Geoscience Union, SSS26-P27.
- Somei, K., M. Miyakoshi and K. Irikura (2014). "Source Model and Strong Ground Simulation for the 2013 Northern Tochigi Prefecture, Japan, Earthquake," Japan Geoscience Union, SSS23-P19 (in Japanese).
- Somei, K., K. Miyakoshi, K. Yoshida, Y. Matsumoto, T. Takahama, S. Kurahashi and K. Irikura (2015a). "Source Modelling and Characterization toward the Strong Ground Motion Prediction for Inland Crustal Earthquakes in Japan," Proceedings of International Workshop on Best Practice in Physics-based Fault Rupture Models for Seismic Hazard Assessment of Nuclear Installations, IAEA, P34.
- Somei, K., K. Miyakoshi and S. Kurahashi (2015b). "Source Model of the 2013 Awaji Island Earthquake (M_w 5.8) derived from Strong Motion Records," Japan Geoscience Union, SS15-P05 (in Japanese).
- Somerville, P., K. Irikura, R. Graves, S. Sawada, D. Wald, N. Abrahamson, Y. Iwasaki, T. Kagawa, N. Smith and A. Kowada (1999). "Characterizing Crustal Earthquake Slip Models for the Prediction of Strong Ground Motion," *Seism. Res. Lett.*, **70**, 59-80.
- Suzuki, W. and T. Iwata (2006). "Source Model of the 2005 West Off Fukuoka Prefecture Earthquake estimated from the Empirical Green's Function Simulation of Broadband Strong Motions," *Earth Planets Space*, **58**, 99-104.
- Yamamoto, Y. and H. Takenaka (2009). "Source Modeling of the 2007 Niigataken Chuetsu-Oki Earthquake using the Empirical Green's Function Method," *ZISIN2 (J. Seismol. Soc. Jpn.)*, **62**, 47-59 (in Japanese).

5th IASPEI / IAEE International Symposium: Effects of Surface Geology on Seismic Motion
August 15-17, 2016

Yoshida, S., T. Kagawa and T. Noguchi (2016). "Difference in Ground Motion Characteristics between the Surface and Buried Rupture Crustal Earthquake in Japan," Japan Geoscience Union, SCG61-P03.

Yoshimi, M. and K. Yoshida (2008). "Site Amplification and Strong Ground Motion of the 2007 Noto Hanto, Japan, Earthquake Estimated from Aftershock Observation," *Earth Planets Space*, **60**, 161-167.